N-Methylfulleropyrrolidine-Based Multimode Sensor for Determination of Butoconazole Nitrate

Bianca-Maria Ţuchiu, Raluca-Ioana Stefan-van Staden,* Jacobus (Koos) Frederick van Staden, and Hassan Y. Aboul-Enein

Read Online

ACCESS | Metrics & More | Article Recommendations | Supporting Information
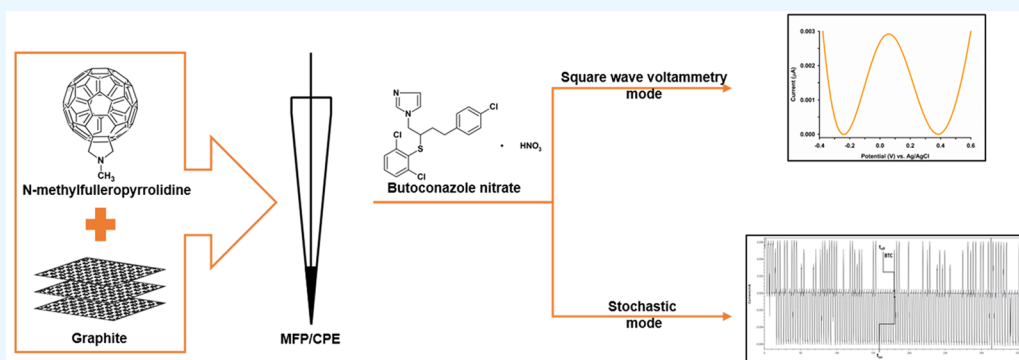
ABSTRACT: A multimode sensor (a sensor responding simultaneously to more than one mode, e.g., stochastic mode, amperometric mode, voltammetric mode) based on graphite paste modified with *N*-methylfulleropyrrolidine was proposed for the determination of butoconazole nitrate in its pharmaceutical formulation. The stochastic mode and square wave voltammetry mode were applied for the determinations. Both the stochastic mode and square wave voltammetry mode were applied for a qualitative and quantitative assay of butoconazole nitrate. The sensor can be used between 1.68×10^{-6} and 1.68×10^{4} μmol L^{-1} when the stochastic mode is used and between 0.168 and 16.80 μmol L^{-1} when the square wave voltammetry mode is used. The multimode sensor was reliably used for the determination of butoconazole nitrate in its pharmaceutical formulation, Gynofort cream, the recorded recoveries being higher than 99.00%, with RSD (%) values of lower than 2.00%.

INTRODUCTION

Butoconazole (BTC, ($\pm$)1-[4-(4-chlorophenyl)-2-(2,6-dichlorophenyl)sulfanylbutyl]imidazole) is an imidazole derivative, part of the azole antifungal drugs class. Its nitrate salt (Figure 1) is used in pharmaceutical formulations such as creams for the local treatment of vulvovaginal fungal infection caused by *Candida* species. BTC is usually well tolerated, with mild adverse effects occurring at the administration site.[1,2] Studies have revealed minimal absorption from the vagina into the systemic circulation.[3] However, one report showed a possible link between BTC administration and severe reversible thrombocytopenia, caused either by BTC cream treatment or by an interaction among BTC, ibuprofen, and methotrexate.[4]

The compendial assay method provided in the United States Pharmacopoeia endorses the determination of butoconazole nitrate in its pure state and its pharmaceutical formulation (vaginal cream) using high-performance liquid chromatography (HPLC) with UV detection.[5] A literature survey revealed several other methods proposed for the determination of BTC from various matrices such as pure form, human plasma and urine, rat plasma and tissue, cream, and water samples. These methods include ultraperformance liquid chromatography (UPLC) with UV detection,[6] reversed-phase liquid chromatography (RPLC) with UV detection,[7] high-
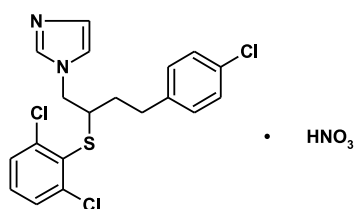
Figure 1. Chemical structure of butoconazole nitrate.

performance thin-layer chromatography (HPTLC)-densitometry,[8] fabric phase sorptive extraction-HPLC with photodiode array detection (FPSE-HPLC-PDA),[9] microextraction by packed sorbent-HPLC (MEPS-HPLC-DAD),[10] liquid chromatography-tandem mass spectrometry (LC-MS/MS),[11,12] capillary electrophoresis (CE),[13] and spectrophotometry.[14] Since BTC is a chiral molecule, liquid chromatography-electrospray ionization coupled with tandem mass spectrometry (LC-ESI-MS/MS) was proposed to detect its enantiomers.[15,16] Although these methods are reliable and generate accurate results, they have several limitations such as high equipment costs, the consumption of large amounts of solvents, and laborious processes of extraction and separation of target analytes. Therefore, the attention of the scientific community has turned toward electrochemical methods due to their low cost, the simplicity of the principle, and the construction of the sensors as well as the fast, sensitive, and selective response.

The development of electrochemical methods is needed to provide an alternative to standard methods of analysis presented in different pharmacopeias. They could help improve drug quality analysis, expanding to a larger scale, toward the pharmaceutical industry, drug analysis laboratories, and even clinical trials. To our knowledge, no electrochemical method for BTC analysis has been reported to date. Therefore, this paper proposes a multimode sensor based on stochastic and square-wave voltammetry (SWV) modes. An N-methylfulleropyrrolidine (MFP)-modified graphite paste electrode (MFP/GPE) was successfully applied in pharmaceutical formulation samples for the determination of BTC. N-Methylfulleropyrrolidine was selected due to its properties of being a good electrocatalyst (needed for the voltammetric mode) and also its capacity of having the channels needed for stochastic detection.

A multimode electrochemical sensor is an electrode that responds simultaneously to more than one mode (e.g., stochastic mode, amperometric mode, voltammetric mode).[17] To date, several multimode sensors have been developed to detect and quantify hormones, neurotransmitters, biomarkers, endocrine disruptors, and enantiomers in various matrices.[18−22]

Carbon-paste electrodes (CPEs) have been successfully employed as working electrodes in electrochemical analysis due to their stable response, robustness, chemical inertness, low non-Faradaic current, low Ohmic resistance, quickly renewable surface, low cost, and ease of fabrication. Moreover, they can be easily modified by either chemical or physical processes with a wide array of materials and molecules to improve their response and sensitivity to electroactive molecules.[23−26] Graphite is the most common carbon-based conductive material used in CPE construction. Under normal temperature and pressure conditions, it is the most stable allotrope of carbon and has important characteristics in terms of electric conductivity, thermal stability, and chemical inertness.[27] Electrochemical sensors have proved to be powerful tools when they are used for pharmaceutical analysis.[28−31]

Fullerenes are a class of stable and hydrophobic molecules made up entirely of carbon atoms arranged in pentagonal, hexagonal, or heptagonal rings. Fullerenes can take spherical, ellipsoidal, or tubular shapes depending on the number of rings. The most used are those comprised of 60 π carbon atoms (C_{60} fullerenes). C_{60} consists of 12 pentagonal and 20

hexagonal rings in which carbon atoms are linked by single and conjugated double bonds, thus forming a symmetrical truncated-icosahedral closed-cage shape. Due to the mixed sp^2 and sp^3 bonds, C_{60} has a high electron affinity, promoting its reduction while hindering oxidation. Fullerene materials are suitable for electrochemical analysis due to their good physical (size, hydrophobicity), electrochemical (electronic configuration), and optical properties.[32] Fulleropyrrolidines are a class of chemically functionalized C_{60} molecules that exhibit higher conductivity and are water-soluble. They are obtained through the Prato reaction, in which azomethine ylides are added to a [6,6] junction of the C_{60} in a 1,3-dipolar cycloaddition. This addition of the pyrrolidine ring transforms the C_{60} into an n-type semiconductor.[33,34]

■ EXPERIMENTAL SECTION

Materials and Reagents. Butoconazole nitrate, N-methylfulleropyrrolidine, graphite powder (<20 μm, synthetic), methanol, monosodium phosphate, disodium phosphate, sodium nitrate, sodium chloride, potassium nitrate, potassium chloride, D-sorbitol, glycerol, EDTA disodium salt, DL-histidine, sodium benzoate, lidocaine, and fusidic acid were purchased from Sigma-Aldrich (Milwaukee, USA); paraffin oil (d_4,[20] 0.86 g cm$^{−1}$) was obtained from Fluka (Buchs, Sweden).

A phosphate buffer solution (PBS, 0.1 mol L$^{−1}$) was prepared using monosodium phosphate and disodium phosphate. Using different quantities of 0.1 mol L$^{−1}$ NaOH or HCl solutions, the pH of the buffer solution was adjusted to obtain various pHs (2.0, 2.5, 3.0, 3.5, 4.0, 4.5, 5.0, and 5.5). The stock solution of 4.21×10^4 μmol L$^{−1}$ butoconazole nitrate was prepared in methanol.

Apparatus and Methods. Electrochemical measurements (cyclic voltammetry (CV), square wave voltammetry (SWV), electrochemical impedance spectroscopy (EIS), and stochastic) were carried out using an EmStat Pico mini potentiostat connected to a laptop with PSTrace software version 5.8 (PalmSens BV, Houten, The Netherlands) for data acquisition. A regular three-electrode system was constructed using MFP/GPE, an Ag/AgCl wire (1 mol L$^{−1}$ KCl), and a Pt wire as the working electrode, reference electrode, and counter electrode, respectively. A Mettler Toledo pH meter was used for the pH adjustment.

All measurements were performed at room temperature.

Design of the MFP/GPE Sensor. The MFP/GPE electrochemical sensor was prepared by physically mixing 100 mg of graphite powder with 20 mg of MFP and an adequate quantity of paraffin oil for 15−20 min until a homogeneous paste was obtained. The paste was inserted into a plastic tube, and an Ag wire served as an electrical contact. Before each measurement, the electrode was cleaned with deionized water. The MFP/GPE surface was renewed by polishing on aluminum foil until a smooth surface was achieved. The sensor was stored at room temperature, in a dry place away from light when not in use.

Procedures. *Stochastic Mode.* The chronoamperometry technique was employed to determine t_{on} and t_{off} values. All measurements were performed at a constant potential of 1.36 V vs Ag/AgCl, which was found to be optimal. Standard solutions of various BTC concentrations were used to calibrate the sensor. The t_{off} value (BTC signature) read in the diagrams served for the qualitative analysis, whereas the t_{on} value was found to be related to the BTC concentration through the calibration equation of the sensor[35]

$$1/t_{on} = a + b \times C_{BTC} \qquad (1)$$

where a is the intercept and b is the slope/sensitivity.

The calibration equation was obtained by applying the linear regression method. The unknown BTC concentration in the sample was calculated by introducing the t_{on} values in the calibration equation.

Square-Wave Voltammetry. All SWV measurements were carried out at a potential domain ranging from −500 to +800 mV, a step potential of 25.0 mV s^{-1}, a 100 mV modulation amplitude, and a frequency of 5.0 Hz. The calibration curve was obtained by plotting BTC concentrations ranging from 0.168 to 16.80 μmol L^{-1} against their corresponding peak heights with a correlation coefficient of above 0.997. Baseline correction was applied to the SWV peaks.

Samples. The proposed electrochemical sensor was used for the BTC determination in its pharmaceutical formulation, Gynofort cream, using stochastic and square-wave voltammetric methods. Besides BTC as the active pharmaceutical ingredient, Gynofort contains the following excipients: sorbitol, propylene glycol, disodium edetate, liquid paraffin, polyglyceryl-3-oleate, glyceryl monoisostearate, microcrystalline wax, hydrophobic colloidal silicon dioxide, methyl *p*-hydroxybenzoate (E 218), propyl *p*-hydroxybenzoate (E 216), and purified water.

For the stochastic mode, the sample was analyzed without any pretreatment in 10 different aliquots taken from the Gynofort. For the voltammetric mode, a weighed amount of 50 mg of the cream was transferred to a 100 mL volumetric flask and treated with ethanol for complete BTC dissolution; 0.1 mol L^{-1} KNO$_3$ (supporting electrolyte) and PBS pH 2.5 were added. Ten solutions were prepared in this way using different aliquots taken from Gynofort.

RESULTS AND DISCUSSION

Electrochemical Characterization of the Sensor. The bare (GPE) and modified (MFP/GPE) electrodes were electrochemically characterized using cyclic voltammetry (CV) and electrochemical impedance spectroscopy (EIS) techniques. The electrochemical response of the MFP/GPE was studied using the CV method. The CVs (Figure S1A) were recorded in a 5.0 × 10^{-3} mol L^{-1} K$_3$[Fe(CN)$_6$] (0.1 mol L^{-1} KCl) solution in a potential range of −0.6 to +1.0 V, at a scan rate of 0.1 V s^{-1}, employing the GPE and MFP/GPE as working electrodes. The modified sensor showed an increased conductivity in comparison with the bare sensor, indicating that the modification with MFP improved the electrochemical response.

The interface of the bare and modified electrodes was investigated through the EIS technique, in the frequency range between 10^5 and 10^{-1} Hz. The measurements were performed in a 5.0 × 10^{-3} mol L^{-1} K$_3$[Fe(CN)$_6$] (0.1 mol L^{-1} KCl) solution. In Figure S1B,C are shown the Nyquist and Bode plots, respectively, recorded for GPE (red line) and MFP/GPE (blue line). The Randles equivalent circuit was chosen to fit the EIS data. This circuit is among the simplest and most commonly used circuits to describe simple electrochemical systems associated with interface/electrolyte processes. As can be observed in the Nyquist plot, GPE presented a large and well-defined semicircle in a low-frequency range, corresponding to high electrical resistance (R_{ct} = 1.055 × 10^6 Ω). After the modification of GPE with MFP, a semicircle with a smaller diameter (R_{ct} = 2.522 × 10^4 Ω) was recorded. The decrease in

the semicircle diameter and R_{ct} value indicates that MFP/GPE yields a faster electron transfer rate. The EIS results are in good agreement with CV measurements.

The electrochemical behavior of the GPE and MFP/GPE was also studied by employing the SWV technique in pH 2.5 PBS containing 0.1 mol L^{-1} KNO$_3$ as the supporting electrolyte and 6.72 μmol L^{-1} BTC. As shown in Figure S1D, MFP/GPE gave better BTC oxidation results than GPE.

Using the Randles−Sevcik equation[36] for quasi-reversible redox processes controlled by diffusion, the electrocatalytic activity of the sensors was studied by calculating the electroactive surface area. The anodic and cathodic peak current intensities are directly proportional to the square root of the scan rate as

$$I_p = \pm(2.69 \times 10^5)n^{3/2}AC_0D_R^{1/2}\nu^{1/2} \qquad (2)$$

where I_p is the peak current (μA), n is the number of transferred electrons (in this case n = 1), A is the electrode active surface area (cm^2), C_0 is the concentration of K$_3$[Fe(CN)$_6$] (mol cm^{-3}), D_R is the diffusion coefficient (7.60 × 10^{-6} cm^2 s^{-1}), and ν is the scan rate (V s^{-1}). The "+" notation corresponds to I_{pa},while "−" corresponds to I_{pc}. The measurements (Figure S2A) were performed in a 5 × 10^{-3} mol L^{-1} K$_3$[Fe(CN)$_6$] (0.1 mol L^{-1} KCl) solution. For the bare and modified electrodes, both the anodic and cathodic peaks (I_{pa} and I_{pc}) showed a linear dependence on the square root of the scan rate, indicating a diffusion-controlled redox process. The linear dependence of I_{pa} and I_{pc} vs $\nu^{1/2}$ is presented in Figure S2B. By applying the Randles−Sevcik equation, the MFP/GPE presented a larger electroactive area, 0.0015 cm^2, compared to 0.0010 cm^2 recorded for the GPE.

Optimization of the pH Values and the Supporting Electrolyte. The influence of pH and supporting electrolytes on BTC oxidation were investigated to optimize the working conditions. For the pH influence study, solutions of PBS at various pH values ranging from 2.0 to 5.5 containing 0.168 μmol L^{-1} BTC were analyzed. As can be observed in Figure S3A, the highest oxidation peak of BTC was obtained in an acidic medium (pH 2.5). Accordingly, pH 2.5 PBS was used for all further measurements. As presented in Figure S3B, the peak potential decreases linearly from pH 2.0 to 5.5 according to the linear relation E_{pa} = 0.18 − 0.05 × pH, with a good regression coefficient (R^2 = 0.9999). The value of the slope is close to the Nernstian theoretical value (0.059 V pH^{-1}), which indicates that the number of protons involved in the electrochemical reaction is equal to the number of electrons.

The supporting electrolyte influence on the electrooxidation of BTC was studied by separately adding 0.1 mol L^{-1} NaCl, KCl, NaNO$_3$, and KNO$_3$ in pH 2.5 PBS containing 0.168 μmol L^{-1} BTC. As can be observed in Figure S3C, the highest peak current was recorded when 0.1 mol L^{-1} KNO$_3$ was used. Thus, all further BTC working solutions were prepared using 0.1 mol L^{-1} KNO$_3$ as supporting electrolyte.

Response Characteristics of the Sensor in the Stochastic Mode. Stochastic sensing is a two-step process based on channel conductivity. In the first step, the analyte flows through the channel and blocks it (the amount of time while the channel is blocked is called t_{off} and represents the signature of the analyte) and the current drops to 0. In the second step, the analyte binds to the channel wall (a process characterized by the t_{on} parameter) and an equilibrium equation takes place

Table 1. Response Characteristics of the MFP/GPE Sensor in Stochastic Mode

calibration eq and correlation coeff (r)	linear concentration range(μmol L^{-1})	t_{off} (s)	sensitivity (s^{-1} mol L^{-1})	LOQ (μmol L^{-1})
$1/t_{on} = 0.13 + 221.64 \times C_{BTC}$, $r = 0.9999$	1.68×10^{-6} to 1.68×10^{4}	1.2	221.64	1.68×10^{-6}

Scheme 1. Proposed Mechanism for Butoconazole Oxidation
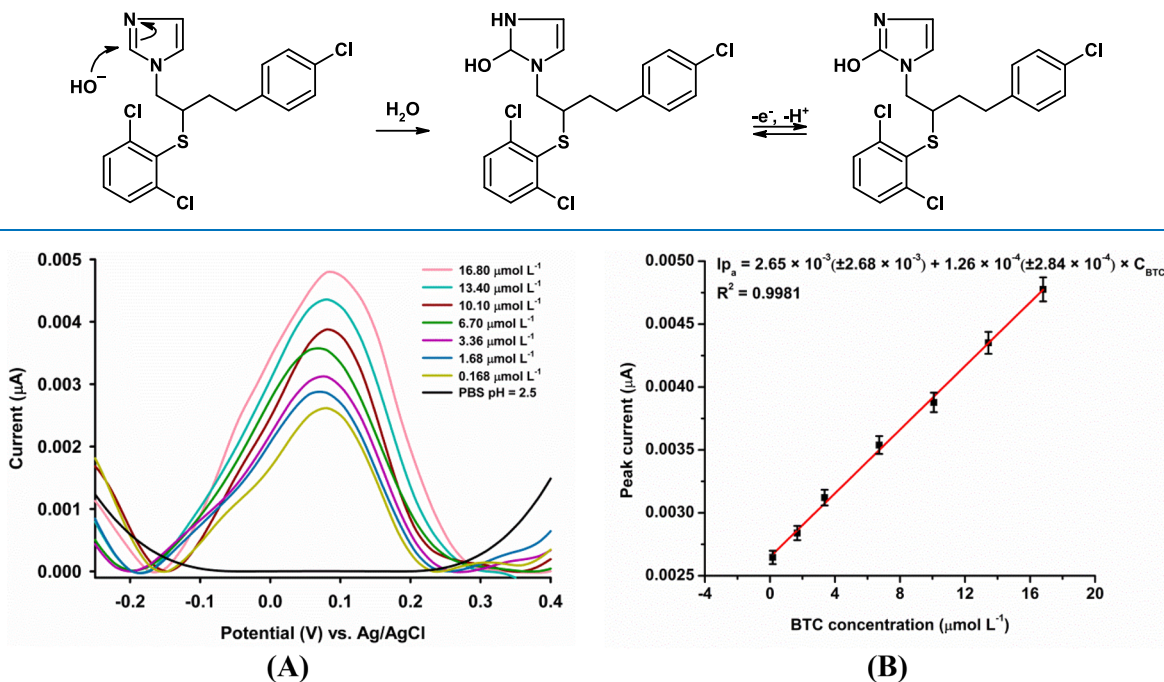
Figure 2. (A) SWVs recorded with MFP/GPE in pH 2.5 PBS containing 0.1 mol L^{-1} KNO$_3$ as the supporting electrolyte and different concentrations of BTC ranging between 0.168 and 16.80 μmol L^{-1}. (B) Calibration curve obtained with MFP/GPE in the linear concentration range from 0.168 to 16.80 μmol L^{-1} BTC. The blank curve was obtained in pH 2.5 PBS.

$$Ch_{(i)} + BTC_{(i)} \Leftrightarrow Ch \cdot BTC_{(i)} \tag{3}$$
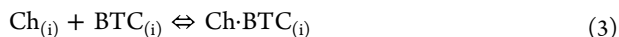
where Ch is the channel and I is the interface.[37]

Table 1 presents the response characteristics of the MFP/GPE sensor. A linear concentration range from 1.68×10^{-6} to 1.68×10^{4} μmol L^{-1} BTC and a limit of quantification (LOQ) of 1.68×10^{4} μmol L^{-1} BTC were obtained when the MFP/GPE sensor was employed in the stochastic mode. The calibration curve is presented in Figure S4. When these results were correlated with the high sensitivity obtained, it could be concluded that the sensor can be used for the BTC analysis in pharmaceutical samples without any pretreatment. This method could prove useful when purity tests are performed on the active pharmaceutical ingredient and also for quality control of its pharmaceutical formulation, Gynofort, and can be applied for uniformity content tests of BTC pharmaceutical formulations.

Response Characteristics of the Sensor in Square-Wave Voltammetry Mode. To determine the response characteristics of the sensor in square wave voltammetry the influence of the scan rate on the electrooxidation of butoconazole nitrate had to be determined. The electrochemical behavior of BTC was studied by the CV technique, using the MFP/GPE at various scan rates ranging from 0.005 to 0.07 V s^{-1}. The CVs were recorded in pH 2.5 PBS containing 0.1 mol L^{-1} KNO$_3$ as supporting electrolyte and 0.168 μmol L^{-1} BTC. The anodic and cathodic peak currents increased with an increase in the scan rate, as presented in Figure S5A.

A linear correlation between the peak current and the square root of the scan rate ($\nu^{1/2}$) (Figure S5B) was observed, as given by the regression equation:

$$I_{pa} = -0.0003 + 0.0059 \times \nu^{1/2} \quad R^2 = 0.9969 \tag{4}$$

A linear dependence was observed when the logarithm of current intensity was plotted against the logarithm of the scan rate (Figure S5C). Their relationship is characterized by the regression equation $\log I_{pa} = -2.01 + 0.73 \times \log \nu$ ($R^2 = 0.9973$). A slope of 0.50 indicates a diffusion-controlled process, while a slope of 1.00 represents a process controlled by adsorption. Furthermore, obtaining an intermediate value suggests a mixed diffusion−adsorption process.[38] Therefore, the calculated slope value of 0.73 indicates a mixed diffusion−adsorption process of BTC with the MFP/GPE surface.

To determine the heterogeneous rate constant, the Laviron equation was used:[39]

$$E_{pa} = E^\circ - \left(\frac{RT}{\alpha nF}\right) \ln\left(\frac{RTk_s}{\alpha nF}\right) + \left(\frac{RT}{\alpha nF}\right) \ln \nu \tag{5}$$

where E° is the formal potential (V), R is the universal gas constant (8.314 J mol^{-1} K^{-1}), T is the absolute temperature (298.15 K), α is the electron transfer coefficient of the BTC oxidation, n is the number of electrons transferred, F is Faraday's constant (96485 C mol^{-1}), k_s is the heterogeneous rate constant of the electrochemical reaction (s^{-1}), and ν is the scan rate (V s^{-1}). The formal potential of BTC ($E^\circ = 0.17$) is

the intercept value of the regression equation obtained by plotting the peak potential against the scan rate:

$$E_{pa} = 0.17 + 4.00 \times \nu \quad R^2 = 0.9734 \tag{6}$$

The oxidation peak potential shifts positively with the increase of the scan rate, as depicted in Figure S5D.

Figure S5E presents the linear dependence of the anodic peak potential on the natural logarithm of the scan rate given by the regression equation

$$E_{pa} = 0.58 + 0.08 \times \ln \nu \quad R^2 = 0.9523 \tag{7}$$

By using the intercept and the slope values from this equation, the heterogeneous rate constant of the electrochemical reaction was calculated to be 0.07 s^{-1}. The kinetic parameters α and n were calculated to be 0.60 and 0.80 ($\sim$1 electron), respectively. Thus, the electrooxidation of BTC involves one electron and one proton, as described in Scheme 1.

The response characteristics of the MFP/GPE toward the BTC oxidation were investigated. SWVs were recorded in pH 2.5 PBS containing 0.1 mol L^{-1} KNO$_3$ as supporting electrolyte and various concentrations of BTC (Figure 2A). By plotting the peak current response against the concentration of BTC (Figure 2B), a linear dependence is observable in the range between 0.168 and 16.80 μmol L^{-1}, characterized by the following regression equation:

$$I_{pa} = 2.65 \times 10^{-3} + 1.26 \times 10^{-4}(\pm 2.84 \times 10^{-4})$$
$$\times C_{BTC} \quad R^2 = 0.9981, \ n = 10 \tag{8}$$

According to the equation, the sensitivity (m) was 1.26 $\times$ 10^{-4} μA μmol L^{-1}. The calculated LOQ and limit of detection (LOD) were determined as per ICH guidelines, by applying the following equations: LOQ = 10s/m and LOD = 3s/m, where s is the standard deviation of the peak current of the blank (five measurements) and m is the slope of the calibration curve.[40,41] Accordingly, the LOQ and LOD were 0.168 and 5 $\times$ 10^{-2} μmol L^{-1}, respectively. The proposed sensor was further assessed using validation parameters such as repeatability, reproducibility, and precision. Table 2 presents the parameters of the calibration curve.

Table 2. Parameters of the Calibration Curve

parameter	value
linear range (μmol L^{-1})	0.168–16.80
intercept (μA)	2.65 $\times$ 10^{-3}
sensitivity (μA μmol L^{-1})	1.26 $\times$ 10^{-4}
correlation coeff	0.9981
LOQ (μmol L^{-1})	0.168
LOD (μmol L^{-1})	5 $\times$ 10^{-2}
no. of data points	7
RSD of the slope (%)	2.84 $\times$ 10^{-4}
RSD of the intercept (%)	2.68 $\times$ 10^{-3}
reproducibility of the peak current (RSD %)	3.87
reproducibility of the peak potential (RSD %)	6.10

A wider linear concentration range as well as a lower limit of quantification were obtained in the stochastic mode. In comparison with classical methods (FPSE-HPLC-PDA),[9] the proposed methods showed wider linear concentration ranges (0.168 and 16.80 μmol L^{-1} in SWV mode and 1.68 $\times$ 10^{-6} to 1.68 $\times$ 10^4 μmol L^{-1} in stochastic mode vs 0.21–16.84 μmol L^{-1} for FPSE-HPLC-PDA) and lower LOQs (0.168 μmol L^{-1} in SWV mode and 1.68 $\times$ 10^{-6} μmol L^{-1} in stochastic mode vs 0.21 μmol L^{-1} for FPSE-HPLC-PDA).

Interference Studies. The effect of seven possible interfering molecules was studied under optimum conditions using the MFP/GPE. The following organic species were selected as possible interfering species in the determination of BTC: D-sorbitol, glycerol, DL-histidine, fusidic acid, EDTA disodium salt, lidocaine, and sodium benzoate.

Interference Studies in Stochastic Mode. In stochastic mode, the selectivity of MFP/GPE toward BTC is determined by the t_{off} parameter values (signature) recorded for the possible interfering molecule. Table 3 presents the individual signatures obtained for the selected molecules when MFP/GPE is usedin stochastic mode. The values obtained proved a high selectivity of the sensor and enabled its use in pharmaceutical samples.

Interference Studies Using SWV Mode. The study was performed byemploying the SWV technique in pH 2.5 PBS containing 0.1 mol L^{-1} KNO$_3$ as supporting electrolyte, 6.72 μmol L^{-1} BTC, and various concentrations of one of the selected interfering species. The experimental results revealed no major changes in the current intensity of BTC for 100-fold excesses of D-sorbitol, glycerol, histidine, and fusidic acid, 50-fold excesses of EDTA disodium salt and lidocaine, and a 10-fold excess of sodium benzoate. Moreover, there was no notable shift of the peak potential when the possible interfering species were analyzed together with a constant concentration of BTC. Figure 3 presents the ratio (I/I_0) between the peak
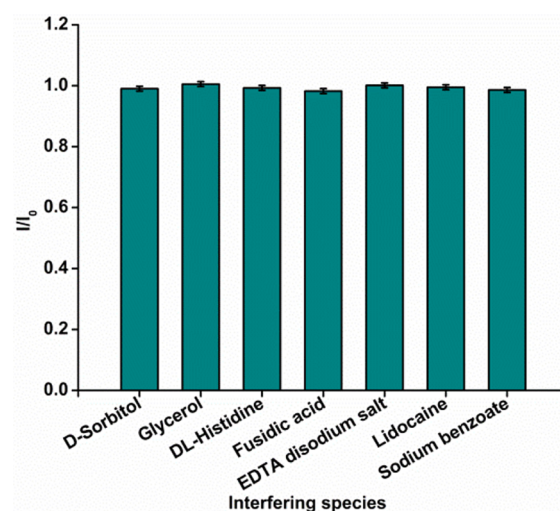
Figure 3. Interference study results of the MFP/GPE sensor used in SWV mode.

Table 3. Selectivity of the Multimode Sensor MFP/GPE in the Stochastic Mode

	interfering species						
	D-sorbitol	glycerol	EDTA disodium salt	DL-histidine	sodium benzoate	lidocaine	fusidic acid
t_{off} (s)	0.3	0.8	2.2	1.6	0.5	1.0	2.0

(A)

(B)
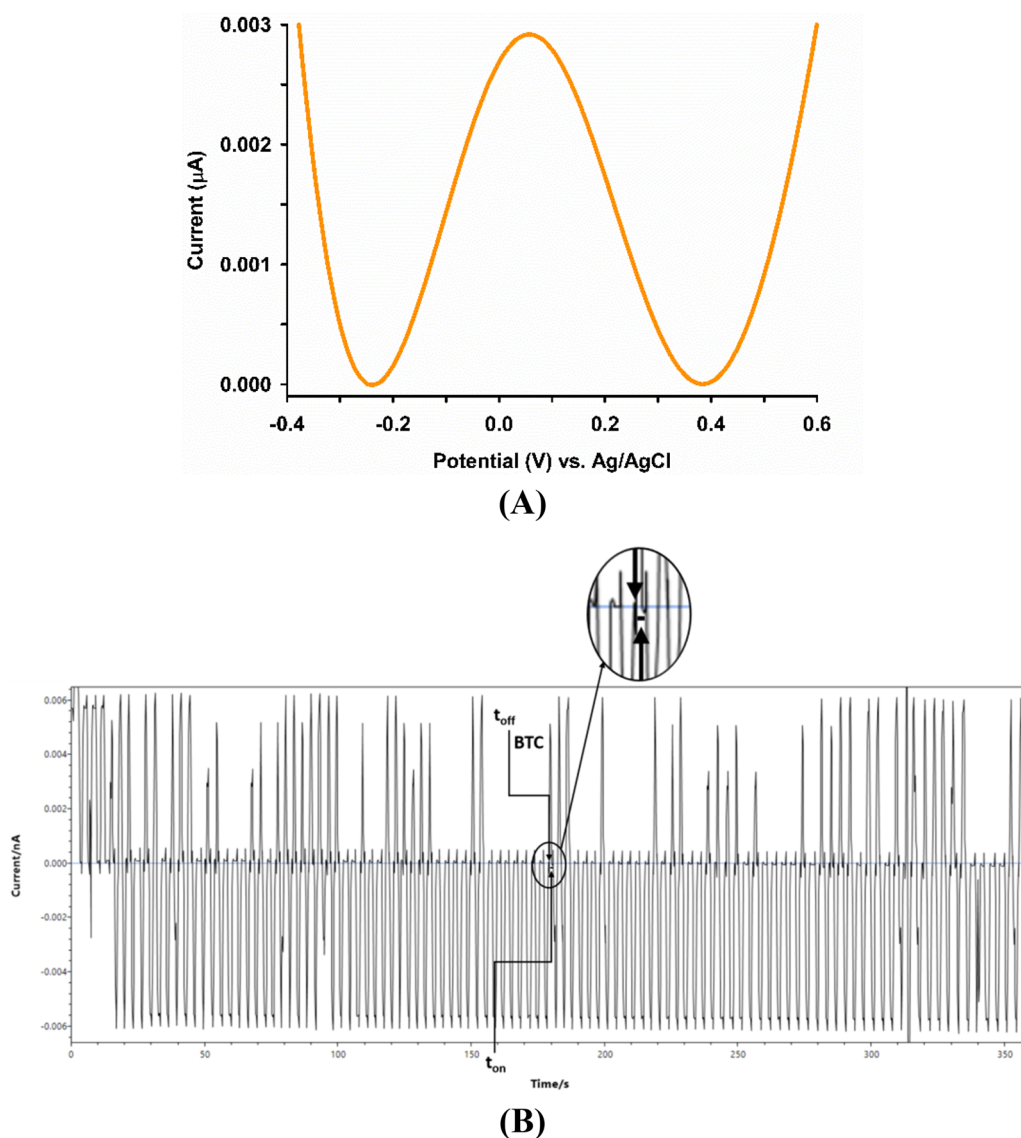
Figure 4. Diagrams obtained using MFP/GPE for the determination of BTC in Gynofort using (A) SWV mode and (B) stochastic mode.

current of BTC in the presence of one of the interfering molecules and the peak current of BTC. As can be seen, the ratio value is close to 1, meaning that the selected molecules did not interfere with BTC detection.

The investigation proved that the proposed sensor presents a high selectivity toward BTC detection when it is employed in the SWV mode. The high sensitivity at low concentrations as well as the high selectivity of the proposed sensor is due to the electrocatalytic activity of MFP; MFP electrocatalyst selectivity is very high for BTC, meaning that it favors the redox processes of BTC, while no electrocatalytic activity was recorded for D-sorbitol, glycerol, DL-histidine, fusidic acid, EDTA disodium salt, lidocaine, and sodium benzoate.

No interference from the substances that may be found in the pharmaceutical formulations was recorded in any of the modes used for BTC determination.

Reproducibility, Repeatability, and Stability. The reproducibility, repeatability, and stability of the MFP/GPE sensor were tested using a solution of BTC (6.72 μmol L^{-1}) under the optimum working conditions, in the SWV mode. To assess the reproducibility, three modified sensors were prepared in a like manner and tested. The relative standard

deviation (RSD%) obtained was 1.34% ($n = 5$). For one of the sensors, the measurement repeatability was studied, giving an RSD value of 1.14% ($n = 6$). The stability of the MFP/GPE was evaluated after it was stored at room temperature, in a dry place. After 2 weeks, the current intensity of BTC was retained at around 90.27 $\pm$ 3.98% compared with the initial response. The supporting voltammograms for reproducibility, repeatability, and stability are represented in Figure S6.

The multimode sensor stability was also investigated when it was used in the stochastic mode for 3 months. The responses obtained were consistent during this period with no major changes concerning the sensitivity of the sensor (RSD% was lower than 1.00%).

Determination of Butoconazole Nitrate in Gynofort Vaginal Cream. The applicability of the proposed multimode sensor was investigated in Gynofort, a pharmaceutical vaginal cream sample containing BTC, using both SWV and stochastic modes.

For the SWV mode, the 10 samples prepared according to the principle previously described were introduced one by one into the electrochemical cell and the peak current was recorded (Figure 4A). By replacing the value of the peak current into the

calibration equation, the BTC concentrations in samples were determined. Table 4 shows the results of the BTC assay in

Table 4. Determination of BTC in Gynofort Vaginal Cream (20 mg/g Butoconazole Nitrate) Using MFP/GPE in SWV Mode[a]

	BTC (μmol L^{-1})				
sample	declared amount	found amount	BTC recovery (%)	RSD (%)	bias (%)
Gynofort 1	2.10	2.11	100.68	0.09	−0.68
Gynofort 2	2.10	2.19	104.33	0.85	−4.15
Gynofort 3	2.10	2.17	103.37	1.27	−3.26
Gynofort 4	2.10	2.10	99.83	1.98	0.17
Gynofort 5	2.10	2.21	105.35	0.04	−5.35
Gynofort 6	2.10	2.14	101.96	1.17	−1.92
Gynofort 7	2.10	2.14	102.07	1.35	−2.03
Gynofort 8	2.10	2.00	95.39	1.14	4.83
Gynofort 9	2.10	2.11	100.68	0.05	−0.68
Gynofort 10	2.10	2.08	99.08	0.03	0.93

[a]All measurements are the average of five determinations.

pharmaceutical samples. The calculated recoveries range from 95.39% to 105.35% with the RSD (%) and bias (%) ranging from 0.03% to 1.98% and from −5.35% to 4.83 %, respectively.

For the stochastic mode, the sample was analyzed without any pretreatments or dilutions, as the concentration of the active substance BTC is within the linear concentration range of MFP/GPE. Thus, the proposed sensor was used for the qualitative and quantitative analysis of BTC in Gynofort. First, the BTC signature was identified in the diagram (Figure 4B), subsequently, the t_{on} value was read and used, as described above in the stochastic mode paragraph, for the determination of BTC concentration. The results obtained are presented in Table 5.

Table 5. Determination of BTC in Gynofort Vaginal Cream (20 mg/g Butoconazole Nitrate) Using MFP/GPE in Stochastic Mode[a]

	BTC (mg/g)				
sample	declared amount	found amount	BTC recovery (%)	RSD (%)	bias (%)
Gynofort	20	19.82 ± 0.03	99.10	0.01	0.90

[a]All measurements are the average of ten determinations.

The results obtained using both modes indicate that the proposed sensor can be reliably used for a qualitative and quantitative reliable analysis of BTC in real samples with minimum interference from the excipients contained by the cream. Additionally, the stochastic mode enables a uniformity content test of the cream without any processing of the sample.

CONCLUSIONS

A multimode sensor based on a functionalized C_{60} fullerene and graphite paste was proposed for a butoconazole nitrate assay in Gynofort. Low and very low limits of determinations were obtained using the stochastic mode and square-wave voltammetry mode, respectively. The sensor presented high sensitivities in both modes, and it was reliable when it was employed for the determination of butoconazole nitrate in real samples. The features of the sensor are its utilization in the pharmaceutical industry for the quality control of butoconazole

nitrate, as well as for a uniformity content assay of its pharmaceutical formulations.

ASSOCIATED CONTENT

Ⓢ Supporting Information

The Supporting Information is available free of charge at https://pubs.acs.org/doi/10.1021/acsomega.2c05904.

Additional figures as described in the text obtained during characterization of the proposed multimode sensor (PDF)

AUTHOR INFORMATION

Corresponding Author

Raluca-Ioana Stefan-van Staden − *Laboratory of Electrochemistry and PATLAB, National Institute of Research for Electrochemistry and Condensed Matter, 060021 Bucharest-6, Romania; Faculty of Chemical Engineering and Biotechnologies, Politehnica University of Bucharest, 060042 Bucharest, Romania;* Ⓘ orcid.org/0000-0001-8244-2483; Phone: +40751507779; Email: ralucavanstaden@gmail.com

Authors

Bianca-Maria Țuchiu − *Laboratory of Electrochemistry and PATLAB, National Institute of Research for Electrochemistry and Condensed Matter, 060021 Bucharest-6, Romania; Faculty of Chemical Engineering and Biotechnologies, Politehnica University of Bucharest, 060042 Bucharest, Romania;* Ⓘ orcid.org/0000-0003-0379-0880

Jacobus (Koos) Frederick van Staden − *Laboratory of Electrochemistry and PATLAB, National Institute of Research for Electrochemistry and Condensed Matter, 060021 Bucharest-6, Romania*

Hassan Y. Aboul-Enein − *Pharmaceutical and Medicinal Chemistry Department, the Pharmaceutical and Drug Industries Research Division, National Research Centre, Cairo 12311, Egypt*

Complete contact information is available at:
https://pubs.acs.org/10.1021/acsomega.2c05904

Notes

The authors declare no competing financial interest.

ACKNOWLEDGMENTS

REFERENCES

(1) Waugh, C. D.Butoconazole. *xPharm: The Comprehensive Pharmacology Reference*; Elsevier: 2007; pp 1−4.

(2) Tatum, D. M.; Eggleston, M. Butoconazole Nitrate. *Infect. Control Hosp. Epidemiol.* **1988**, *9*, 122−124.

(3) Adamson, G. D. Three-Day Treatment of Vulvovaginal Candidiasis. *Am. J. Obstet. Gynecol.* **1988**, *158*, 1002−1005.

(4) Maloley, P. A.; Nelson, E.; Montgomery, H. A.; Campbell, J. R. Severe Reversible Thrombocytopenia Resulting from Butoconazole Cream. *DICP* **1990**, *24*, 143−144.

(5) *The United States Pharmacopeia and National Formulary* (USP 43-NF 38), 2020.

(6) Pattanaik, P.; Subrahmanyam, K. V. UPLC Method development and validation for butoconazole in active ingredient. *Int. J. Pharm. Res. Health Sci.* **2015**, *3*, 15−21.

(7) Üstün, Z.; Çubuk-Demiralay, E. Simultaneous Quantitative Determination of Imidazole Antimycotics in Human Urine by Using RPLC Technique. *Eurasian J. Anal. Chem.* **2017**, *12*, 953−962.

(8) Sayed, R. A.; Elmasry, M. S.; Hassan, W. S.; El-Mammli, M. Y.; Shalaby, A. Development and application of degradation kinetics of thin layer chromatographic densitometry and conductometric methods for butoconazole nitrate determination. *Ann. Pharm. Fr.* **2018**, *76*, 453−463.

(9) Locatelli, M.; Kabir, A.; Innosa, D.; Lopatriello, T.; Furton, K. G. A fabric phase sorptive extraction-high performance liquid chromatography-photo diode array detection method for the determination of twelve azole antimicrobial drug residues in human plasma and urine. *J. Chromatogr. B* **2017**, *1040*, 192−198.

(10) Campestre, C.; Locatelli, M.; Guglielmi, P.; De Luca, E.; Bellagamba, G.; Menta, S.; Zengin, G.; Celia, C.; Di Marzio, L.; Carradori, S. Analysis of imidazoles and triazoles in biological samples after microextraction by packed sorbent. *J. Enzyme Inhib. Med. Chem.* **2017**, *32*, 1053−1063.

(11) Nouman, E. G.; Al-Ghobashy, M. A.; Lotfy, H. M. Development and validation of LC-MS/MS assay for the determination of butoconazole in human plasma: evaluation of systemic absorption following topical application in healthy volunteers. *Bull. Fac. Pharm. Cairo Univ.* **2017**, *55*, 303−310.

(12) Jia, M. M.; Zhou, Y.; He, X. M.; Wu, Y. L.; Li, H. Q.; Chen, H.; Li, W. Y. Development of a liquid chromatography-tandem mass spectrometry method for determination of butoconazole nitrate in human plasma and its application to a pharmacokinetic study. *J. Huazhong Univ. Sci. Technol. Med. Sci.* **2014**, *34*, 431−436.

(13) Senchenko, S. P.; Checheneva, K. S.; Gavrilin, M. V.; Ushakova, L. S. Butoconazole nitrate pharmacokinetics studied by capillary electrophoresis. *Pharm. Chem. J.* **2009**, *43*, 597−600.

(14) Zayed, M. A.; El-Shal, M. A.; Azime, M. A. Spectrophotometric determination of fluconazole, voriconazole and butoconazole nitrate by ion-pair formation with Rose bengal reagent. *Egypt. J. Chem.* **2017**, *60*, 5−8.

(15) Wang, Z.; Zhao, P.; Yu, J.; Jiang, Z.; Guo, X. Experimental and molecular docking study on graphene/Fe_3O_4 composites as a sorbent for magnetic solid-phase extraction of seven imidazole antifungals in environmental water samples prior to LC-MS/MS for enantiomeric analysis. *Microchem. J.* **2018**, *140*, 222−231.

(16) Ma, S.; Wang, L.; Guo, G.; Yu, J.; Guo, X. Solid phase extraction procedure coupled with the chiral LC-ESI-MS/MS method for the enantioseparation and determination of butoconazole enantiomers in rat plasma and tissues: application to the enantioselective study on pharmacokinetics and tissue distribution. *New J. Chem.* **2021**, *45*, 1317−1326.

(17) Gugoasa, L. A.; Stefan-van Staden, R. I. Advanced methods for the analysis of testosterone. *Curr. Med. Chem.* **2018**, *25*, 4037−4049.

(18) Gugoasa, L. A.; Stefan-van Staden, R. I.; Calenic, B.; Legler, J. Multimode sensors as new tools for molecular recognition of testosterone, dihydrotestosterone and estradiol in children's saliva. *J. Mol. Recognit.* **2015**, *28*, 10−19.

(19) Stefan-van Staden, R. I.; Moldoveanu, I.; van Staden, J. F. Pattern recognition of neurotransmitters using multimode sensing. *J. Neurosci. Methods* **2014**, *229*, 1−7.

(20) Gugoasa, L. A.; AI Ogaidi, A. J. M.; Stefan-van Staden, R. I.; El-Khatib, A.; Rosu, M. C.; Pruneanu, S. Multimode microsensors based on Ag−TiO_2−graphene materials used for the molecular recognition of carcinoembryonic antigen in whole blood samples. *RSC Adv.* **2017**, *7*, 28419−28426.

(21) Stefan-van Staden, R. I.; Moldoveanu, I. Multimode sensors based on nanostructured materials for simultaneous screening of biological fluids for specific breast cancer and Hepatitis B biomarkers. *J. Electroch. Soc.* **2014**, *161*, B45.

(22) Stefan-van Staden, R. I.; Comnea-Stancu, I. R. Chiral single-walled carbon nanotubes as chiral selectors in multimode enantioselective Sensors. *Chirality* **2021**, *33*, 51−58.

(23) Karimi-Maleh, H.; Karimi, F.; Rezapour, M.; Bijad, M.; Farsi, M.; Beheshti, A.; Shahidi, S.-A. Carbon paste modified electrode as powerful sensor approach determination of food contaminants, drug ingredients, and environmental pollutants: A Review. *Curr. Anal. Chem.* **2019**, *15*, 410−422.

(24) State-Georgescu, R.; van Staden, J. F.; State, R. N.; Papa, F. Rapid and sensitive electrochemical determination of tartrazine in commercial food samples using IL/AuTiO₂/Go composite modified carbon paste electrode. *Food Chem.* **2022**, *385*, 132616.

(25) State-Georgescu, R.; van Staden, J. F. Review. Electrochemical sensors used in the determination of L-Dopa. *Electrochem. Sci. Adv.* **2021**, *2*, No. e2100040.

(26) Comnea-Stancu, I. R.; van Staden, J. F.; Stefan-van Staden, R.-I. Facile detection of naphthalene with a 5,10,15,20-tetrakis(4-methoxyphenyl)-21H,23H-porphine nickel (II)/N-(1-naphthyl) ethylenediamine dihydrochloride renewable graphene oxide paste electrode. *J. Electrochem. Soc.* **2022**, *169*, No. 037527.

(27) Nahirny, E. P.; Bergamini, M. F.; Marcolino-Junior, L. H. Improvement in the performance of an electrochemical sensor for ethanol determination by chemical treatment of graphite. *J. Electroanal. Chem.* **2020**, *877*, 114659.

(28) Jayaprakash, G. K.; Swamy, B. E. K.; Rajendrachari, S.; Sharma, S. C.; Flores-Moreno, R. Dual descriptor analysis of cetylpyridinium modified carbon paste electrods for ascorbic acid sensing applications. *J. Mol. Liq.* **2021**, *334*, 116348.

(29) Kudur Jayaprakash, G.; Swamy, B.E. K.; Sanchez, J. P. M.; Li, X.; Sharma, S.C.; Lee, S.-L. Electrochemical and quantum chemical studies of cetylpyridinium bromide modified electrode interface for sensor applications. *J. Mol. Liq.* **2020**, *315*, 113719.

(30) Jayaprakash, G. K.; Flores-Moreno, R. Quantum chemical study of Triton x-100 modified graphene surface. *Electrochim. Acta* **2017**, *248*, 225−231.

(31) Kudur Jayaprakash, G.; Swamy, B.E. K.; Casillas, N.; Flores-Moreno, R. Analytical Fukui and cyclic voltametric studies on ferrocene modified carbon electrodes and effect of Triton X-100 by immobilization method. *Electrochim. Acta* **2017**, *258*, 1025−1034.

(32) Kurbanoglu, S.; Ozkan, S. A. Electrochemical carbon based nanosensors: A promising tool in pharmaceutical and biomedical analysis. *J. Pharm. Biomed. Anal.* **2018**, *147*, 439−457.

(33) Richardson, M. C.; Park, E. S.; Kim, J. H.; Holmes, G. A. N-pyrrolidine functionalized C_{60}-fullerenes/epoxy nanocomposites. *J. Appl. Polym. Sci.* **2010**, *117*, 1120−1126.

(34) Peyghan, A. A.; Soleymanabadi, H.; Moradi, M. Structural and electronic properties of pyrrolidine-functionalized [60]fullerenes. *J. Phys. Chem. Solids* **2013**, *74*, 1594−1598.

(35) Stefan-van Staden, R.-I.; Ilie-Mihai, R.-M.; Gheorghe, D.-C.; Bogea, I. M.; Badulescu, M. 2D disposable stochastic sensors for molecular recognition and quantification of maspin in biological samples. *Microchim. Acta* **2022**, *189*, 101.

(36) Zanello, P.*Inorganic electrochemistry*; Royal Society of Chemistry: 2007.

(37) Gheorghe, D.-C.; Ilie-Mihai, R.-M.; Stefan-van Staden, R.-I.; Lungu-Moscalu, A.; van Staden, J. F. Fast screening method for early diagnostic of gastric cancer based on utilization of a chitosan − S-doped graphene - based needle stochastic sensors. *J. Pharm. Biomed. Anal.* **2022**, *214*, 114725.

(38) Gosser, D. K.*Cyclic Voltammetry: Simulation and Analysis of Reaction Mechanisms*; Wiley-VCH: 1994.

(39) Laviron, E. General expression of the linear potential sweep voltammogram in the case of diffusionless electrochemical systems. *J. Electroanal. Chem. Interfacial Electrochem.* **1979**, *101*, 19−28.

(40) *Analytical Method Development and Validation*, 1st ed.; Swartz, M. E.; Krull, I. S., Eds.; Marcel Dekker: 1997.

(41) ICH Q2 (R1) Validation of analytical procedures: text and methodology. https://database.ich.org/sites/default/files/Q2%28R1%29%20Guideline.pdf (August 2022).